MedChemComm

CONCISE ARTICLE

View Article Online
View Journal

Cite this: DOI: 10.1039/c4md00409d

The effect of *N*-methylation on transition state mimetic inhibitors of the *Plasmodium* protease, plasmepsin V†

Michelle Gazdik,[ab] Matthew T. O'Neill,[ab] Sash Lopaticki,[ab] Kym N. Lowes,[ab] Brian J. Smith,[c] Alan F. Cowman,[ab] Justin A. Boddey[ab] and Brad E. Sleebs*[ab]

Received 15th September 2014
Accepted 24th November 2014

DOI: 10.1039/c4md00409d

www.rsc.org/medchemcomm

N-Methylation of the N–Cα peptide bond is a known strategy to overcome the liabilities inherently associated with peptide-like molecules. Here, we apply this strategy to transition state mimetics that are potent inhibitors of the malarial protease, plasmepsin V, with the aim of enhancing their activity against *Plasmodium* parasites. We demonstrate that independent *N*-methylation of each N–Cα bond of the mimetics interferes with binding interactions to plasmepsin V, resulting in reduced affinity for the protease. We provide evidence that *N*-methylation improves proteolytic stability and slightly improves lipophilicity. However, the observed parasite activity of the *N*-methyl compounds had little correlation with on-target plasmepsin V activity, indicating non-specific activity. This study underscores the benefits and the drawbacks of the *N*-methylation strategy, and provides further evidence that plasmepsin V is highly sensitive to substrate modification.

Introduction

Malaria is caused by infection with *Plasmodium* parasites. Each year, *Plasmodium* parasites cause several hundred million infections and over 650 000 human deaths.[1] Combination drug therapies have proved effective in reducing the disease burden. However, the current arsenal of clinically used artemisinin combination therapies, and promising drug candidates undergoing clinical assessment, may not be sufficient in effectively eliminating the disease due to the threat of emerging resistance. This highlights an urgent need for the development of new antimalarial therapies.

To survive within erythrocytes, parasites deliver proteins into the host cell, using protein export mechanisms, to remodel the infected erythrocyte and its surface (reviewed in ref. 2–4). The majority of proteins destined for export to the erythrocyte possess an N-terminal pentameric motif known as the *Plasmodium* export element (PEXEL; RxLxQ/E/D)[5] or vacuolar transport signal.[6] The PEXEL motif is proteolytically processed in the parasite's endoplasmic reticulum (ER)[7,8] by Plasmepsin V (PMV),[9,10] an ER-resident, membrane-bound aspartic acid protease.[11] Processing by PMV is an essential step for export of PEXEL-containing proteins and for parasite survival in human erythrocytes.[12] PMV and PEXEL proteins are conserved in all *Plasmodium* spp.[13]

Cleaved PEXEL proteins exit the ER and are trafficked across the parasite membrane and parasitophorous vacuole membrane through the PTEX complex (the *Plasmodium* translocon of exported proteins)[14–16] to reach the host cell.

Recently, transition state (TS) mimetics of the natural PEXEL substrate were shown to be potent inhibitors of PMV from *P. falciparum* and *P. vivax*, and to impair protein export in *P. falciparum*-infected erythrocytes, killing the parasites.[12,17] The most potent PMV inhibitor to date, WEHI-916, has high affinity for the PMV enzyme (19 nM IC_{50}), and an EC_{50} of 2.5 μM against *P. falciparum* cultured in human erythrocytes.[12,17] The marked decrease in efficacy in culture may be linked to the peptide-like nature of WEHI-916.

One strategy to overcome the liabilities associated with peptide-like compounds is *N*-methylation of the backbone amide bonds.[18–20] This approach has been shown to reduce proteolytic degradation[21–24] and aid in cell membrane permeability.[24–26] In some instances, this has led to improved cellular potency.[24,27–29] Herein, we describe the generation of a set of analogues delineated from an *N*-methyl scan of the peptide backbone of previously described TS mimetics that are potent inhibitors of PMV. We used the approach to independently probe the amide bond conformational rigidity and hydrogen bonding requirements of the mimetics with PMV. The analogues provide evidence that highlight the advantages and disadvantages of *N*-methylation as a strategy to overcome the

[a]*The Walter and Eliza Hall Institute of Medical Research, Parkville, 3052, Australia. E-mail: sleebs@wehi.edu.au; Tel: +61 3 9345 2718*

[b]*Department of Medical Biology, The University of Melbourne, Parkville, 3010, Australia*

[c]*Department of Chemistry, La Trobe University, 3086, Australia*

† Electronic supplementary information (ESI) available: Experimental for chemistry, molecular modeling and biology. Compound dose response curves for the PMV biochemical assay, the *P. falciparum* viability assay and results of the serum stability assay. See DOI: 10.1039/c4md00409d

liabilities inherently associated with peptide-like small molecules.

Results and discussion

Chemistry

We selected compound **1** (Fig. 1), previously described in Sleebs *et al.*,[17] as the progenitor compound on which to conduct the *N*-methyl scan. The mimetic **1** inhibited PMV with an IC_{50} value of 0.35 μM, and in addition reduced parasite viability in culture with an EC_{50} of 15 μM. It is known from previous studies[12,17] that compound **1** possesses key attributes that are required for inhibition of PMV. The P_3 Arg of **1** makes key interactions in the S_3 pocket of PMV and is critical for binding affinity. The P_1 Leu that occupies the S_1 pocket of PMV was found to be highly sensitive to modification. The S_2 pocket of PMV tolerates a variety of amino acids, however, mimetics with a Val, Ile or Leu were shown to give the highest binding affinity.[12,17] For the purpose of this study, the *N*-methyl compounds **2–5** were proposed, based on the parent compound **1** that possessed a P_2 Ala, as depicted in Fig. 1. In addition to **1**, a more potent inhibitor of PMV that possessed a P_2 Val, **6**, (analogous to WEHI-916 (ref. 12 and 17)) and its *N*-methyl surrogate, **7**, were also prepared (Fig. 1).

There are a plethora of methods to synthesise *N*-methyl amino acids present in the literature,[30] however, many of these methods result in racemization of the α-centre of the amino acid, are not compatible with peptide protection group strategies, or result in incomplete *N*-methylation. A high yielding approach that overcomes these shortfalls is the use of the 5-oxazolidinone scaffold. This methodology has not only allowed the generation of all proteinaceous α-amino acids, but also a range of unnatural amino acids.[31–38] We sought to apply this technology to the synthesis of *N*-methyl amino acids used in the *N*-methyl scan.

To construct the peptide-like analogues that incorporated the *N*-methyl amino acids, solution phase synthesis was employed. The synthesis of the progenitor compound **1** and the *N*-methyl C-terminal N–H compound, **5**, were produced using a similar synthetic scheme to that of Sleebs *et al.*,[17] as shown in Scheme 1. Briefly, Cbz-Arg(*N*,*N*-diBoc)-OH **8**, was coupled to alanine ethyl ester. The ester **9** was then hydrolysed to obtain **10**. The acid **10** was then coupled to the statine amides **14** and **15**, to give the respective products **17** and **18**. Finally, Boc-deprotection gave the desired compounds **1** and **5**.

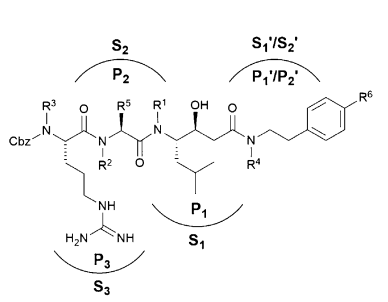

	R^3	R^2	R^1	R^4	R^5	R^6
1	H	H	H	H	Me	Cl
2	Me	H	H	H	Me	Cl
3	H	Me	H	H	Me	Cl
4	H	H	Me	H	Me	Cl
5	H	H	H	Me	Me	Cl
6	H	H	H	H	*i*Pr	H
7	H	Me	H	H	*i*Pr	H

Fig. 1 The P_3 to P_2' regions of **1** and the associated binding pockets of PMV (S_3–S_2'). The inset table describes the proposed *N*-methyl scan.

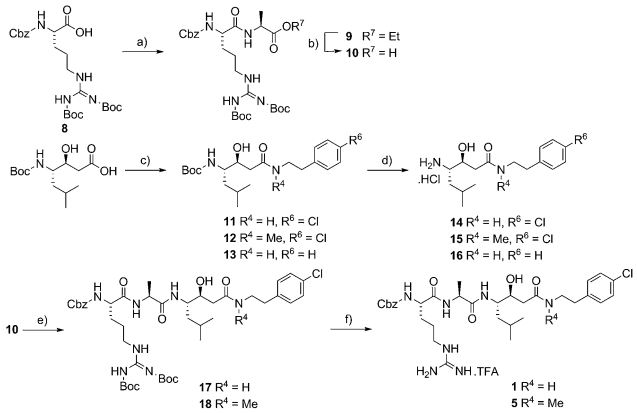

Scheme 1 Synthesis of analogues **1** and **5**. *Reagents and conditions*: (a) HCl·NH_2–Ala–OEt, HBTU, DIPEA, DMF, 18 h; (b) LiOH, THF, H_2O, 5 min; (c) 2-(4-chlorophenyl)-ethylamine for **11**; 2-(4-chlorophenyl)-*N*-methyl ethanamine for **12**; phenylethylamine for **13**; HBTU, DIPEA, DMF, 18 h; (d) 4 N HCl in dioxane, 1 h; (e) **14** for **17**; **15** for **18** HBTU, DIPEA, DMF, 18 h; (f) TFA, DCM, 18 h.

The *N*-methyl Ala and *N*-methyl Val methyl ester, **19** and **20**, were produced using the previously described oxazolidinone strategy[31–34] and were independently coupled to Cbz-Orn(*N*-Boc)-OH **21**. The resulting methyl esters **23** and **25** were hydrolysed to obtain **27** and **29**, respectively, which were coupled to the statine amide **14** to give the respective products **30** and **32**. The *N*-Boc protection group was then removed under acidic conditions, and reacted with *N*,*N*′-bis-Boc-1-guanylpyrazole to form the guanidine moieties **33** and **35**. Boc-deprotection gave rise to the desired *N*-methyl Ala analogue **3** and the *N*-methyl Val analogue **7**. The synthesis of the non-methylated

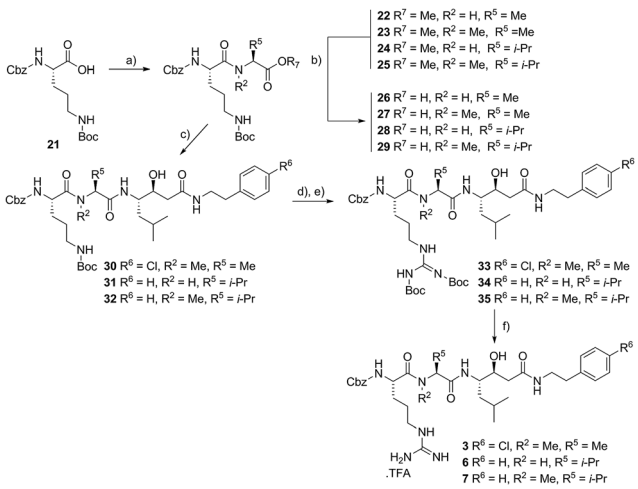

Scheme 2 Synthesis of **3**, **6** and **7**. *Reagents and conditions*: (a) HCl·NH_2–Ala–OMe for **22**; HCl·$NH(CH_3)$–Ala–OMe **19** for **23**; HCl·NH_2–Val–OMe for **24**; HCl·$NH(CH_3)$–Val–OMe **20** for **25**; HBTU, DIPEA, DMF, 18 h; (b) LiOH, THF, H_2O; (c) **14** for **30**; **16** for **31** and **32**; HBTU, DIPEA, DMF, 18 h; (d) 4 N HCl in dioxane, 1 h; (e) *N*,*N*′-bis-Boc-1-guanylpyrazole, Et_3N, DCM, 18 h; (f) TFA, DCM, 18 h.

valine analogue **6** was also produced following this pathway, as shown in Scheme 2.

We next wanted to generate the *N*-methyl Arg analogue. However, directly accessing *N*-methyl Arg from arginine using the oxazolidinone technology is problematic, and therefore a modified synthesis starting from a protected Orn was utilised, previously described by Aurelio and Sleebs *et al.*[31,33] Cbz-Orn(*N*-Phth)-OH **36**, was converted to the *N*-methyl amino acid **38** *via* the oxazolidinone **37**. This allowed for coupling of the dipeptide **40** to the protected *N*-methyl Orn **36** generating the tripeptide **41**. The *N*-Phth protection group was removed from **41** using hydrazine hydrate and the resultant free amine was subsequently reacted with *N*,*N*′-bis-Boc-1-guanylpyrazole to install the protected guanidine moiety. Boc deprotection of **42** yielded the desired *N*-methyl Arg analogue **2** (Scheme 3).

The synthesis of the *N*-methyl statine has been previously described by Wagner *et al.*[39,40] This method is similar to that utilising the oxazolidinone to produce *N*-methyl amino acids, however, the key intermediate is an oxazolidine. The synthesis was initiated with protecting the carboxylic acid of Boc-statine **43** as a benzyl ester; this step prevented the preferential formation of the lactone when forming the oxazolidine. The oxazolidine intermediate **44** was formed smoothly using paraformaldehyde with a catalytic quantity of PTSA. The benzyl ester was then hydrolysed to form the acid **45**, which was then coupled to 2-(4-chlorophenyl)-ethylamine to produce the amide **46**. Concomitant Boc-deprotection and reductive cleavage was then performed generating the *N*-methyl statine **47**. However, in this reaction we observed that 20% de-formylation of the iminium intermediate had occurred shown by the integration of the N–Me peak in the ^{1}H-NMR spectrum. Despite this, **47** was then used in the coupling reaction with the dipeptide **26** to produce the tripeptide **48**. The side chain of the ornithine in the tripeptide **48** was then deprotected under acidic conditions, and reacted with *N*,*N*′-bis-Boc-1-guanylpyrazole to install the guanidine functionality affording **49**. Removal of the Boc-protection gave the desired *N*-methyl statine analogue **4** (Scheme 4).

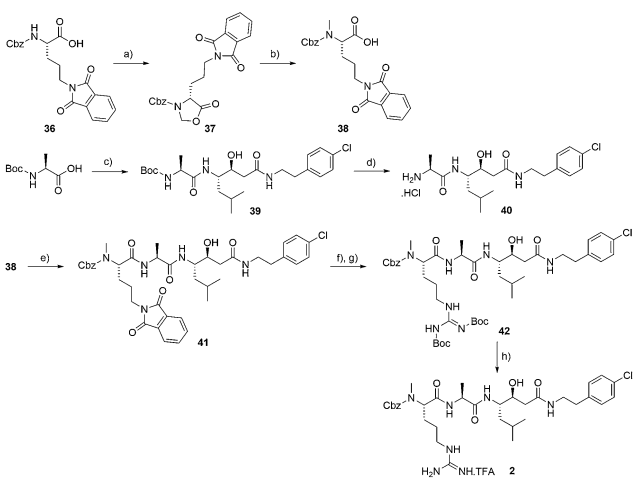

Scheme 3 Synthesis of the *N*-methyl arginine analogue **2**. *Reagents and conditions*: (a) PTSA, paraformaldehyde, toluene, 90 °C, 3 h; (b) Et_3SiH, TFA, DCM, 18 h; (c) **14**, HBTU, DIPEA, DMF, 18 h; (d) 4 N HCl in dioxane, 1 h; (e) **40**, TFFH, DIPEA, DMF, 18 h; (f) $N_2H_4 \cdot H_2O$, EtOH, 18 h; (g) *N*,*N*′-bis-Boc-1-guanylpyrazole, Et_3N, DCM, 18 h; (h) DCM, TFA, 18 h.

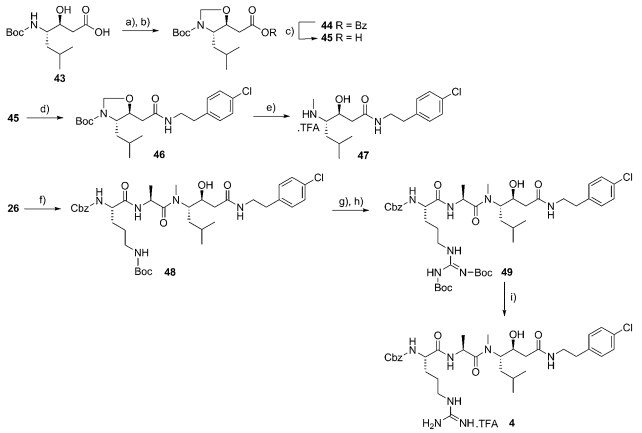

Scheme 4 Synthesis of the *N*-methyl statine analogue **4**. *Reagents and conditions*: (a) Benzyl bromide, K_2CO_3, DMF, 3.5 h; (b) PTSA, paraformaldehyde, toluene, 90 °C, 4 h; (c) LiOH, THF, H_2O, 18 h; (d) 2-(4-chlorophenyl)-ethylamine, HBTU, DIPEA, DMF, 18 h; (e) Et_3SiH, TFA, DCM, 18 h; (f) **47**, HBTU, DIPEA, DMF, 18 h; (g) 4 N HCl in dioxane, 5 h; (h) *N*,*N*′-bis-Boc-1-guanylpyrazole, Et_3N, DCM, 18 h; (i) DCM, TFA, 18 h.

Biological evaluation

To assess whether *N*-methylation of the mimetics affected the inhibitory activity of PMV, the *N*-methyl analogues were assessed and then compared to the activity of **1**. Inhibitory activity was determined using the previously described fluorogenic substrate processing assay that employs a substrate containing the PEXEL sequence RTLAQ from the exported knob-associated histidine-rich protein (KAHRP) with the DABCYL – EDANS fluorophore combination.[9]

The evaluation of compounds against *P. falciparum* PMV revealed that *N*-methylation of every peptide bond N–H was detrimental to activity when compared to **1**. In particular, analogue **3**, which possessed P_2 *N*-methyl Ala, had the greatest reduction in inhibition, with an IC_{50} value of 48 μM. This dramatic reduction in affinity for PMV was also reflected when comparing **7**, which possessed P_2 *N*-methyl Val, to the parent non-methylated analogue **6**. A 50-fold decrease in inhibitory activity was observed with *N*-methylation of the P_1 Arg (**2**), compared to the non-methylated compound **1**. The *N*-methylation of the C-terminal amide (**5**) exhibited a 20-fold reduction in inhibitory activity. However, the *N*-methylation of statine (**4**) was somewhat tolerated with an IC_{50} of 890 nM, and only slightly less potent than the N–H comparator **1** (300 nM IC_{50}) (Table 1).

The reduced inhibitory activity of the compounds in this study likely results from either the loss of essential hydrogen bond interactions of the N–H amide with hydrogen-bond acceptors in the active site of PMV (necessary for the target protein to recognize its ligand) – the concomitant steric clash with the N–Me group – or, restriction of the conformational flexibility about the N–Cα and Cα–C(O) bonds.[41] In a model of

Table 1 Biological activity of the N–H and *N*-methyl analogues

#	R^3	R^2	R^1	R^4	R^5	PMV[a] (±SEM) (μM)	Parasite viability[b] (±SEM) (μM)	HepG2[c] (μM)	*c* log *P*[d]
1	H	H	H	H	Me	0.30 (0.13)	15.3 (0.09)	>50	2.34
2	Me	H	H	H	Me	15.6 (4.1)	67.8 (0.25)	>50	2.57
3	H	Me	H	H	Me	48.0 (7.6)	23.2 (0.52)	>50	2.57
4	H	H	Me	H	Me	0.89 (0.33)	29.2 (0.45)	>50	2.57
5	H	H	H	Me	Me	5.35 (3.3)	20.3 (0.21)	>50	2.57
6	H	H	H	H	*i*Pr	0.026 (0.01)	3.97 (0.17)	>50	2.63
7	H	Me	H	H	*i*Pr	>50	5.89 (0.46)	N.d.	2.85

[a] IC_{50} Data represents means ± SEMs for three fluorogenic substrate cleavage experiments. A 9-point dilution series of each compound was incubated (37 °C) with *P. falciparum* ipPMV-HA. WEHI-916 (ref. 12 and 17) IC_{50} 24 nM. [b] EC_{50} data represents means ± SEMs for three experiments. 7-point dilution series of **1–7** were incubated with *P. falciparum* 3D7 parasites for 72 h. Chloroquine EC_{50} 0.01 μM. [c] EC_{50} data represents means for three experiments in an 11-point dilution series over 48 h. Etoposide EC_{50} 9.8 μM. [d] Calculated using Chemaxon software.[41] N.d. – no data. R^1 to R^5 refers to groups in Fig. 1.

the progenitor non-methylated compound **1** bound to PMV (Fig. 2), Thr312 forms a hydrogen-bond interaction with the N–H of the P_3 Arg of **1**, and may explain why *N*-methylation of the P_3 (**2**) is not tolerated by PMV. Glu136, that makes a key interaction with the guanidine side-chain, forms a hydrogen bond with the N–H of the P_2 alanine of **1**; this P_2 N–H group lies in close proximity to the side-chains of both the P_1 Leu and P_3 Arg. *N*-Methylation of the P_2 alanine (**3**) caused a 160-fold loss in potency. We propose that this loss is not only attributed to the disruption of the N–H interaction with Glu136, but also to perturbing the critical interaction that Glu136 forms with the P_3 Arg of the substrate, and steric clash with the side-chains of these two critical substrate residues.

The reduced activity arising from *N*-methylation of the C-terminal N–H (**5**) can be attributed to the loss of the C-terminal N–H interaction with the backbone carbonyl of Gly77; steric clash of the *N*-methyl with this carbonyl will also likely cause displacement of the amide plane and subsequent loss of the hydrogen bond between the statine carbonyl and the backbone amide of Cys135. The model also suggests that the statine N–H interacts with the backbone carbonyl of Gly310; notably though, *N*-methyl substitution of the statine (**4**) was shown to retain some activity, suggesting this interaction may not be critical. The dramatic loss of activity from *N*-methylation of both the P_3 and P_2 residues further highlights the high sensitivity PMV possesses toward substrate modification.

The improvement in potency of **6** compared to **1**, is suggested by the homology model of PMV in complex with compound **1** (Fig. 2). The model shows that the replacement of the R^5 Me (**1**) with *i*Pr (**6**) would place this group in close proximity to the hydrophobic side-chains of Cys178 and Phe370; improved hydrophobic packing of *i*Pr relative to Me at this site may account for the increased affinity of **6** compared to its parent **1**.

A key benefit of *N*-methylation is improved proteolytic stability. To test whether this was indeed the case with our compounds, the *N*-methyl analogues **2**, **3**, **4** and **5** were compared to their progenitor non-methylated compound **1**, in the presence of a pancreatic extract containing active peptidases and proteases (Fig. 3). We used the pancreatic extract as a surrogate model for emulating the peptidases and proteases that are found in *Plasmodium* parasites. Each compound was incubated in the presence of the pancreatic extract at 37 °C and monitored for proteolytic degradation by LCMS at several time points over 24 h. The study showed that the *N*-methyl analogues

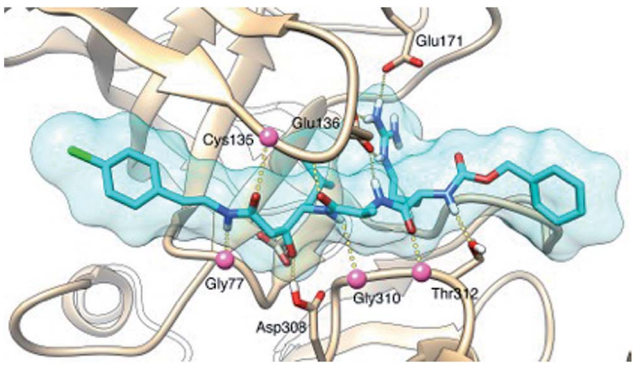

Fig. 2 An interaction diagram showing the key interactions of the backbone amides of **1** (cyan) with PMV (tan), based on the homology model. Hydrogen bonds between the substrate (**1**) and PMV are highlighted with yellow-dotted lines.

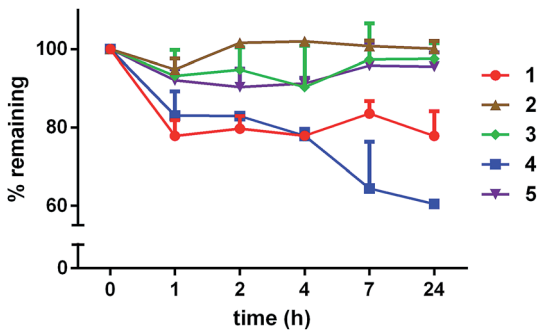

Fig. 3 Stability of the non-methylated compound **1** compared to the *N*-methyl analogues **2**, **3**, **4** and **5**, incubated in the presence of pancreatin in phosphate buffer (pH 7.4) at 37 °C. Data presented are averages of duplicate measurements and expressed as percentages relative to the average concentration of the initial time point. Error + SD.

2, **3** and **5** exhibited improved stability relative to the non-methylated compound **1**. However, the *N*-methyl statine analogue was less stable compared to **1** over 24 h. The stability study suggests that compounds **2**, **3** and **5** may have improved stability in the presence of proteases and peptidases harboured by *Plasmodium* parasites in culture. Analogues **1–5** were all found to be stable in human serum over 55 h (ESI Table S1†).

Another benefit of *N*-methylation is the possibility of enhanced lipophilicity and membrane permeability. *c* log *P* values are shown in Table 1 and demonstrate that there is negligible difference between the lipophilicity of the non-methylated **1** in comparison to the *N*-methyl compounds **2–5** and **6** in comparison to **7**. From the *c* log *P* values, it is unlikely that a small change in lipophilicity would enhance the membrane permeability of the mono *N*-methylated analogues **2–5** and **7**.

There is published evidence that *N*-methylation can improve cellular potency.[24,27–29] As we observed no increase in inhibitory activity against PMV, we predicted that our *N*-methylated compounds were unlikely to have increased potency against parasites in culture, if the compounds were truly specific to PMV. To examine this, compounds **1–7** were assessed in a parasite viability assay described previously.[12,17] *P. falciparum*-infected human erythrocytes were treated with the compounds in 9-point titrations and parasitaemia determined after 72 h by flow cytometry and compared to vehicle-treated controls. Compared to the non-methylated compounds, **1** and **6**, the respective mono *N*-methylated analogues **2–5** and **7**, all exhibited weaker inhibition of parasite growth. This was not unexpected as a loss in PMV affinity was observed for **2–5** and **7** compared to **1** and **6**. It is noted that analogues **2**, **3** and **7** killed parasites (67.8, 23.2 and 5.9 μM EC_{50}, respectively) despite having very weak activity against PMV (15.6, 48.0 and >50 μM IC_{50}, respectively). This is most likely a result of non-specific off-target activity.

To determine whether the inhibition of PMV contributed to the observed parasite activity of compounds **1–7**, we assessed the ability of compounds **1–7** to block processing of the *Plasmodium falciparum* erythrocyte membrane protein 3 (PfEMP3) fused to green fluorescent protein (GFP) in transgenic *P. falciparum* parasites in culture, following an established protocol.[12,17] The processing of the PEXEL in PfEMP3 was assessed by immunoblotting with anti-GFP antibodies. The western blot in Fig. 4 shows that only compounds **1** and **6** were shown to have an effect on PEXEL processing of PfEMP3. Compound **6** was the most effective at blocking processing, which correlated well with compound **6** possessing the most potent biochemical inhibition of PMV (Table 1). Compound **6** was also seen to have a similar effect on processing as the previously described and structurally similar compound, WEHI-916.[12,17] The level of PEXEL-cleaved protein observed did not quantitatively reflect the degree of PMV inhibition by **1**, **6** or WEHI-916, as the inhibitors were added well after PEXEL processing and export of PfEMP3-GFP had initiated. This processing experiment does however, demonstrate target engagement of PMV in *P. falciparum* parasites.

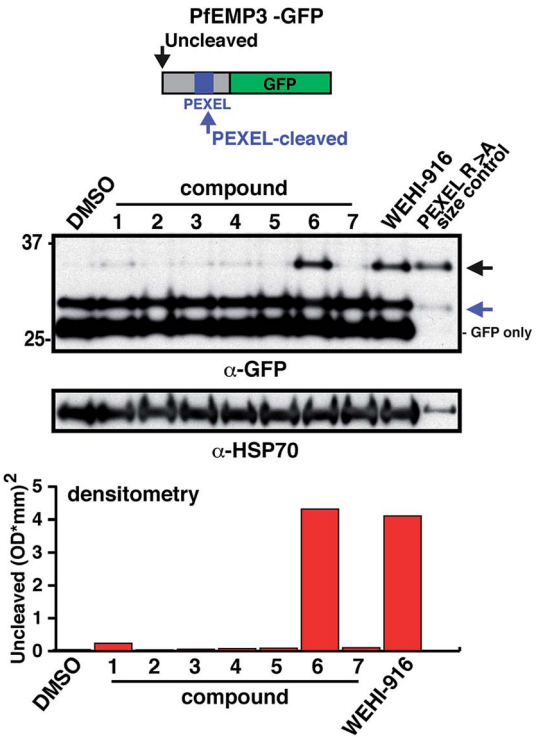

Fig. 4 Activity of selected transition state mimetics against PMV in cultured parasites. *P. falciparum* trophozoites expressing PfEMP3-GFP in infected erythrocytes were treated with 20 μM of compounds **1–7**, WEHI-916 (ref. 12 and 17) or vehicle control (DMSO) and processing of the PEXEL in PfEMP3 was assessed by immunoblotting with anti-GFP antibodies. A schematic of the GFP protein and its cleavage positions is shown at the top. Uncleaved (black arrow), PEXEL-cleaved (blue arrow), and "GFP only" (a degraded remnant of the GFP reporter in the food vacuole) species of PfEMP3-GFP are indicated next to the immunoblot. PEXEL R > A mutant PfEMP3-GFP was included as a size control, and the blot was probed with parasite anti-HSP70 as a loading control. Densitometry of the uncleaved band in each lane is shown beneath the blot.

The *N*-methylated compounds **2–5** and **7** did not have an effect in the PfEMP3 processing assay (Fig. 4). Although The *N*-methylated compounds **2–5** and **7** were shown to kill parasites in culture (Table 1), this was not as a result of engaging PMV, demonstrated by the inability these compounds to effect processing of PfEMP3 (Fig. 4). This demonstrates that the *N*-methylation strategy was not only detrimental to PMV activity and processing of PfEMP3, but also resulted in an increase in non-specific activity as shown by the weak correlation of data from the biochemical and parasite viability assays (Table 1). Additionally, it is difficult to draw conclusions as to whether the marginal improvement in metabolic stability and lipophilicity actually improved parasite activity, due to the lack of affinity of the *N*-methylated compounds, **2–5** and **7**, for PMV.

Conclusions

N-Methylation of the peptide backbone amides is favourably viewed with regard to improving proteolytic stability and permeability in a cellular context.[18–20] However, this study demonstrates that *N*-methylation had profound effects on the

binding affinity for PMV and, hence, inhibitory activity. The PMV homology model provides evidence that reduced inhibitory activity against PMV is likely due to the loss of key interactions with PMV, due to the combination of conformational restriction of the C–Nα bond and the abrogation of crucial hydrogen bond interactions with PMV.

N-Methylation was seen to enhance metabolic stability and marginally increase lipophilicity. However, due to the poor inhibition of PMV *in vitro*, and poor correlation with on-target activity in *P. falciparum* parasites, it was difficult to assess whether these attributes had a positive outcome on improving activity in a cellular context. Moreover, *N*-methylation appeared to enhance the non-specific activity of compounds against parasites in culture, and thus this study alerts peptidomimetic researchers to the potential limitations of *N*-methylation as a strategy to improve cellular activity of peptide-like compounds.

PMV is an essential protease for survival of parasites in the human host. This study shows that *N*-methylation of compounds that potently inhibit PMV reduces their activity, confirming that PMV is highly sensitive to substrate alteration, and illuminates the challenges that lay ahead in the design of peptidomimetics that target PMV.

Acknowledgements

This work was funded by the National Health and Medical Research Council of Australia (Project Grant 1010326 to J.A.B), a CASS Foundation Science and Medicine grant (SM.12.4348 to JAB), the Australian Cancer Research Foundation, the Victorian State Government Operational Infrastructure Support and Australian Government NHMRC IRIISS. We thank the University of Melbourne for the provision of an Australian Postgraduate Award to M.G. A.F.C. is a Howard Hughes International Scholar and an Australia Fellow of the NHMRC. J.A.B is an Australian Research Council QEII Fellow. We thank Guillaume Lessene, Janet Weinstock and Andrew Powell for useful discussions.

Notes and references

1 WHO, *World Malaria Report*, 2013.
2 M. Marti and T. Spielmann, *Curr. Opin. Microbiol.*, 2013, **16**, 445–451.
3 J. A. Boddey and A. F. Cowman, *Annu. Rev. Microbiol.*, 2013, **67**, 243–269.
4 B. Elsworth, B. S. Crabb and P. R. Gilson, *Cell. Microbiol.*, 2014, **16**, 355–363.
5 M. Marti, R. T. Good, M. Rug, E. Knuepfer and A. F. Cowman, *Science*, 2004, **306**, 1930–1933.
6 N. L. Hiller, S. Bhattacharjee, C. van Ooij, K. Liolios, T. Harrison, C. Lopez-Estrano and K. Haldar, *Science*, 2004, **306**, 1934–1937.
7 J. A. Boddey, R. L. Moritz, R. J. Simpson and A. F. Cowman, *Traffic*, 2009, **10**, 285–299.
8 H. H. Chang, A. M. Falick, P. M. Carlton, J. W. Sedat, J. L. DeRisi and M. A. Marletta, *Mol. Biochem. Parasitol.*, 2008, **160**, 107–115.
9 J. A. Boddey, A. N. Hodder, S. Gunther, P. R. Gilson, H. Patsiouras, E. A. Kapp, J. A. Pearce, T. F. de Koning-Ward, R. J. Simpson, B. S. Crabb and A. F. Cowman, *Nature*, 2010, **463**, 627–631.
10 I. Russo, S. Babbitt, V. Muralidharan, T. Butler, A. Oksman and D. E. Goldberg, *Nature*, 2010, **463**, 632–636.
11 M. Klemba and D. E. Goldberg, *Mol. Biochem. Parasitol.*, 2005, **143**, 183–191.
12 B. E. Sleebs, S. Lopaticki, D. S. Marapana, M. T. O'Neill, P. Rajasekaran, M. Gazdik, S. Gunther, L. W. Whitehead, K. N. Lowes, L. Barfod, L. Hviid, P. J. Shaw, A. N. Hodder, B. J. Smith, A. F. Cowman and J. A. Boddey, *PLoS Biol.*, 2014, **12**, e1001897.
13 T. J. Sargeant, M. Marti, E. Caler, J. M. Carlton, K. Simpson, T. P. Speed and A. F. Cowman, *Genome Biol.*, 2006, **7**, R12.
14 T. F. de Koning-Ward, P. R. Gilson, J. A. Boddey, M. Rug, B. J. Smith, A. T. Papenfuss, P. R. Sanders, R. J. Lundie, A. G. Maier, A. F. Cowman and B. S. Crabb, *Nature*, 2009, **459**, 945–949.
15 J. R. Beck, V. Muralidharan, A. Oksman and D. E. Goldberg, *Nature*, 2014, **511**, 592–595.
16 B. Elsworth, K. Matthews, C. Q. Nie, M. Kalanon, S. C. Charnaud, P. R. Sanders, S. A. Chisholm, N. A. Counihan, P. J. Shaw, P. Pino, J. A. Chan, M. F. Azevedo, S. J. Rogerson, J. G. Beeson, B. S. Crabb, P. R. Gilson and T. F. de Koning-Ward, *Nature*, 2014, **511**, 587–591.
17 B. E. Sleebs, M. Gazdik, M. T. O'Neill, P. Rajasekaran, S. Lopaticki, K. Lackovic, K. N. Lowes, B. J. Smith, A. F. Cowman and J. A. Boddey, *J. Med. Chem.*, 2014, **57**, 7644–7662.
18 J. Chatterjee, C. Gilon, A. Hoffman and H. Kessler, *Acc. Chem. Res.*, 2008, **41**, 1331–1342.
19 J. Chatterjee, F. Rechenmacher and H. Kessler, *Angew. Chem., Int. Ed.*, 2013, **52**, 254–269.
20 S. Sagan, P. Karoyan, O. Lequin, G. Chassaing and S. Lavielle, *Curr. Med. Chem.*, 2004, **11**, 2799–2822.
21 F. Haviv, T. D. Fitzpatrick, R. E. Swenson, C. J. Nichols, N. A. Mort, E. N. Bush, G. Diaz, G. Bammert and A. Nguyen, *J. Med. Chem.*, 1993, **36**, 363–369.
22 A. Janecka, R. Kruszynski, J. Fichna, P. Kosson and T. Janecki, *Peptides*, 2006, **27**, 131–135.
23 Y. Linde, O. Ovadia, E. Safrai, Z. Xiang, F. P. Portillo, D. E. Shalev, C. Haskell-Luevano, A. Hoffman and C. Gilon, *Pept. Sci.*, 2008, **90**, 671–682.
24 A. Muppidi, K. Doi, S. Edwardraja, E. J. Drake, A. M. Gulick, H.-G. Wang and Q. Lin, *J. Am. Chem. Soc.*, 2012, **134**, 14734–14737.
25 D. J. Gordon, R. Tappe and S. C. Meredith, *J. Pept. Res.*, 2002, **60**, 37–55.
26 O. Ovadia, S. Greenberg, J. Chatterjee, B. Laufer, F. Opperer, H. Kessler, C. Gilon and A. Hoffman, *Mol. Pharmaceutics*, 2011, **8**, 479–487.
27 E. Biron, J. Chatterjee, O. Ovadia, D. Langenegger, J. Brueggen, D. Hoyer, H. A. Schmid, R. Jelinek, C. Gilon, A. Hoffman and H. Kessler, *Angew. Chem., Int. Ed.*, 2008, **47**, 2595–2599.

28 D. R. Bolin, A. L. Swain, R. Sarabu, S. J. Berthel, P. Gillespie, N. J. S. Huby, R. Makofske, L. Orzechowski, A. Perrotta, K. Toth, J. P. Cooper, N. Jiang, F. Falcioni, R. Campbell, D. Cox, D. Gaizband, C. J. Belunis, D. Vidovic, K. Ito, R. Crowther, U. Kammlott, X. Zhang, R. Palermo, D. Weber, J. Guenot, Z. Nagy and G. L. Olson, *J. Med. Chem.*, 2000, **43**, 2135–2148.
29 K. S. Harris, J. L. Casey, A. M. Coley, J. A. Karas, J. K. Sabo, Y. Y. Tan, O. Dolezal, R. S. Norton, A. B. Hughes, D. Scanlon and M. Foley, *J. Biol. Chem.*, 2009, **284**, 9361–9371.
30 L. Aurelio, R. T. Brownlee and A. B. Hughes, *Chem. Rev.*, 2004, **104**, 5823–5846.
31 L. Aurelio, R. T. C. Brownlee, A. B. Hughes and B. E. Sleebs, *Aust. J. Chem.*, 2000, **53**, 425–433.
32 L. Aurelio, J. S. Box, R. T. C. Brownlee, A. B. Hughes and M. M. Sleebs, *J. Org. Chem.*, 2003, **68**, 2652.
33 A. B. Hughes and B. E. Sleebs, *Helv. Chim. Acta*, 2006, **89**, 2611–2637.
34 A. B. Hughes and B. E. Sleebs, *Aust. J. Chem.*, 2005, **58**, 778.
35 B. E. Sleebs and A. B. Hughes, *J. Org. Chem.*, 2007, **72**, 3340–3352.
36 N. H. Nguyen, B. E. Sleebs, J. M. White and A. B. Hughes, *Tetrahedron*, 2012, **68**, 8068.
37 A. B. Hughes and B. E. Sleebs, *Synth. Commun.*, 2009, **39**, 48–60.
38 B. E. Sleebs, N. H. Nguyen and A. B. Hughes, *Tetrahedron*, 2013, **69**, 6275–6284.
39 B. Wagner, R. Beugelmans and J. Zhu, *Tetrahedron Lett.*, 1996, **37**, 6557–6560.
40 B. Wagner, G. I. Gonzalez, M. E. Tran Hun Dau and J. Zhu, *Bioorg. Med. Chem.*, 1999, **7**, 737–747.
41 Calculator Plugins were used for structure property prediction and calculation, Marvin 14.17.17.10, 2014, ChemAxon, http://www.chemaxon.com.